Polymer Journal, Vol. 17, No. 2, pp 409—419 (1985)

Light Scattering and Sedimentation Equilibrium Study on Concentrated Solutions of a Rodlike Polysaccharide Schizophyllan

Kazuo VAN and Akio TERAMOTO*

Department of Macromolecular Science, Osaka University, Toyonaka, Osaka 560, Japan

(Received September 11, 1984)

ABSTRACT: Light scattering and sedimentation equilibrium measurements were made on concentrated solutions of a rodlike polysaccharide schizophyllan using three samples of different molecular weights. The data were analyzed to obtain the partial derivative $[\partial\Delta\mu_0/\partial\phi]_{Mn}$ of the excess chemical potential of the solvent with respect to the polymer volume fraction ϕ. The results for isotropic solutions were analyzed by the theory of Flory and Abe for rodlike polymers, yielding a non-vanishing interaction parameter χ. For any of the samples investigated, χ was negative and decreased with increasing ϕ. No appreciable dependence of χ on molecular weight was found. Sedimentation measurement was also made on biphasic mixtures consisting of isotropic and cholesteric phases at equilibrium to evaluate $[\partial\Delta\mu_0/\partial\phi]_{Mn}$ at the phase boundary in the two phases. No theory was found to describe precisely our experimental data.

KEY WORDS Chemical Potential / Rodlike Polymer / Polysaccharide / Light Scattering / Sedimentation Equilibrium / Schizophyllan / Interaction Parameter / Flory Theory / Onsager Theory / Thermodynamics /

A solution of a rodlike polymer forms an anisotropic phase at high concentration, and separates into equilibrium isotropic and anisotropic phases at a certain intermediate concentration. Such phase behavior as well as the thermodynamic properties of these phases can in principle be predicted if relevant expressions are available for the chemical potentials of the components involved. The theories so far developed along this line of thought indicate that an asymmetric shape of the polymer is of primary importance for the formation of an anisotropic phase.[1-4] However, it is predicted[1-3] that intermolecular interactions also play an important role in the phase behavior. Thus, knowledge of the chemical potentials is essential for testing theoretically predicted phase relationships. As far as we are aware, attempts to approach such knowledge have been made only by Kubo and Ogino[5,6] who studied the system poly(γ-benzyl L-glutamate) + dimethylformamide. They obtained thermodynamic data that could be compared favorably with the prediction of Cotter's theory.[4] Applicability of this theory to other systems is yet to be seen.

For the reason given below, aqueous schizophyllan, in which this rodlike polysaccharide[7,8] forms a cholesteric mesophase at high concentrations,[9-11] cannot be regarded as an athermal solution of hard rods in a non-interacting medium. The average value of the second virial coefficient for aqueous schizophyllan at 25°C is 1.25×10^{-4} mol cm^3 g^{-2}.[7,8] Analysis of this value by Zimm's theory of rodlike polymers[12] gives 1.2 nm for the diam-

* To whom correspondence should be addressed.

eter of the schizophyllan triple helix. This is smaller than 1.67 nm calculated from the partial specific volume of schizophyllan in water at infinite dilution ($0.619\,cm^3\,g^{-1}$) and the molecular weight per unit length M_L of 2140 nm^{-1} and also smaller than the hydrodynamic diameter 2.2—2.6 nm reported by Norisuye and coworkers.[7,8] These disparities suggest that concentrated aqueous schizophyllan is non-athermal and its thermodynamic properties cannot be described in terms of the geometry of the schizophyllan helix alone. Therefore, we attempted to directly evaluate the thermodynamic properties of aqueous schizophyllan. Thus, light scattering and sedimentation equilibrium measurements were made on isotropic solutions and sedimentation measurement was made on biphasic mixtures. The resulting data were treated according to Scholte[13,14] to obtain the solvent chemical potential. This paper describes the experimental results and their comparison with theoretical predictions.

EXPERIMENTAL

Polysaccharide Samples

Sonicated schizophyllan samples supplied by Taito Co. were purified or separated into many fractions from aqueous solutions with methanol or acetone as the precipitant in our laboratory. Five fractions were chosen from them and designated as SPG-3′ ($M_w=159000$, $M_z/M_w=1.2$), R23 ($M_w=245000$, $M_z/M_w=1.2$), D40 ($M_w=478000$, $M_z/M_w=1.2$), SPG-01 ($M_v=105000$), and E-4 ($M_v=150000$). The molecular weights of these samples were determined by sedimentation equilibrium measurement or viscosity measurement on dilute solutions at 25°C; the intrinsic viscosity $[\eta]-M_w$ relationship of Yanaki *et al.*[8] was used to obtain the viscosity-average molecular weight M_v. For light scattering measurement, sample R23 was dissolved in water at about 1 wt%, filtered through a Millipore filter GSWP0 2500 of pore size 0.22 μm, and freeze-dried.

A required amount of a schizophyllan sample was dried *in vacuo* overnight and mixed with water in a stoppered flask. The mixture became transparent within two days. Dissolution was effected by slowly rotating the flask or by stirring the mixture by a magnetic bar. The polymer weight fraction w was determined gravimetrically except for R23 solutions; those of R23 solutions were determined by refractometry after the light scattering measurement.

Refractive Index and Density Measurements

Refractive indices n for light of the wavelengths 436 and 546 nm were measured on aqueous solutions of the sample E-4 over the polymer concentration range up to 15 wt% at 25°C. A Bausch & Lomb precision sugar refractometer was used. The values of n obtained are plotted against w in Figure 1, where the solid curves follow the data points for the respective wavelengths. Owing to the difficulty in handling highly viscous solutions and a limited amount of the sample available, no sufficient data were obtained to determine the n *vs.* w relationship accurately. Therefore, we searched for appropriate relationships giving an initial slope consistent with the literature specific refractive index increment at infinite

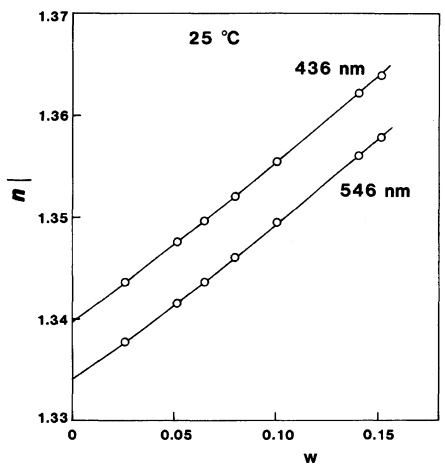

Figure 1. Concentration dependence of refractive index of aqueous schizophyllan at 25°C; solid lines, calculated from eq 1.

dilution[7] and a reasonable n value at $w=1$, *i.e.*, for the pure polymer. The resulting equations are

$$n=1.3339+0.1416w+0.123w^2-0.03124w^3 \quad (546\,\text{nm}) \qquad (1)$$

$$n=1.3397+0.1446w+0.115w^2-0.0243w^3 \quad (436\,\text{nm})$$

Densities of aqueous solutions of sample SPG-01 were measured on a Lipkin–Davison type pycnometer of 5 cm^3 capacity over the concentration range up to 9.5 wt% at 25°C. The data for the specific volume v of isotropic solutions obtained were fitted by the equation:

$$v=1.003-0.384w+0.03w^2 \qquad (2)$$

This was determined by the same method as used in deriving eq 1.

Light Scattering Measurement

A FICA 50 automatic photogoniometer was used with cylindrical cells of 1.8 cm in diameter. Intensities of scattered light were measured for vertically polarized incident light of the wavelengths 546 and 436 nm at scattering angles between 30 and 150°. Appropriate neutral density filters were used to attenuate strong 436 nm intensities. The transmittances of the filters were determined from the ratio of the 90° scattering intensities measured with and without the filter on aqueous schizophyllan or a polystyrene–xylene solution. The photogoniometer was calibrated with benzene according to the procedure established in our laboratory. Test solutions were filtered through a Millipore filter of the pore size 0.22 μm and centrifuged directly in the light scattering cell.

Sedimentation Equilibrium Measurement

Sedimentation equilibrium measurement on isotropic solutions was made by using a Beckman-Spinco Model E analytical ultracentrifuge equipped with a schlieren optical system at 25°C. A Kel-F 12 mm cell or an Epon 30 mm double-sector cell was used and the solution column was adjusted to a length between 0.7 and 1.5 mm. The rotor speed was chosen at 3000—4000 rpm.

For a biphasic mixture, an appropriate volume of it was placed in a Kel-F cell and the whole cell assembly was kept at 30°C at least for two days to effect phase separation. The cell assembly was then loaded on a J-rotor heated at 30°C and centrifuged at a rotor speed between 2000 and 5600 rpm. The length of the solution column was adjusted between 1.5 and 4.3 mm.

TREATMENT OF LIGHT SCATTERING AND SEDIMENTATION EQUILIBRIUM DATA

Consider a solution consisting of a polymer and a single solvent; the polymer may or may not be monodisperse in molecular weight. In a light scattering measurement, vertically polarized light is incident on the solution and the intensity of scattered light is measured as a function of the scattering angle θ to obtain the reduced excess scattering intensity R_θ. The quantity Z_{LS} defined by

$$Z_{LS}=-\frac{RTKM_0wv}{R_0} \qquad (3)$$

can be related to the thermodynamic properties of the solution. Here, R_0 is the value of R_θ extrapolated to the zero scattering angle, M_0 the molecular weight of the solvent,[15] v the specific volume of the solution, and K the optical constant defined by

$$K=\frac{4\pi^2n^2(\partial n/\partial w)^2}{N_A\lambda_0^4} \qquad (4)$$

with N_A the Avogadro number, $\partial n/\partial w$ the specific refractive index increment on the weight fraction basis, and λ_0 the wavelength of incident light *in vacuo*. For a monodisperse solute, Z_{LS} is equal to the partial derivative $[\partial\Delta\mu_0/\partial w]$ of the solvent chemical potential with respect to w at fixed temperature and

pressure.[13,14]

For aqueous schizophyllan, the values of $\partial n/\partial w$ and v as functions of w can be obtained using the relations established (eq 1 and 2). Thus, with the known values of N_A and λ_0, light scattering measurement allows Z_{LS} to be evaluated for isotropic solutions of schizophyllan. In so doing, M_0 was taken to be 2200 for the reason given in the following section.

Next, consider the same polymer solution at sedimentation equilibrium in an ultracentrifuge cell. A sedimentation equilibrium measurement gives the refractive index gradient dn/dr in the solution as a function of the distance r from the center of rotation. A quantity Z_{SED} (essentially the same as Z_{LS}) is obtained from dn/dr by

$$Z_{SED}=\frac{M_0 w(r) r\omega^2(\partial v/\partial w)(\partial n/\partial w)}{v(dn/dr)} \quad (5)$$

where ω is the angular velocity, $w(r)$ the polymer weight fraction at r, and $\partial v/\partial w$ the partial derivative of v with respect to w. When the rotor speed is low and the solution column is short, the concentration gradient developed in the cell is almost constant throughout the entire solution and $w(r)$ at the midpoint of the solution is very close to the weight fraction in the original solution, which is hereafter denoted by w. Thus, the sedimentation equilibrium method allows us to evaluate Z_{SED} for a known w. A similar analysis may be made for phase-separated solutions as well if $w(r)$ at the phase boundary can be determined.

Actually, sedimentation equilibrium measurements on isotropic solutions of schizophyllan were carried out under the conditions specified above and the data were analyzed by eq 5 along with the data for $\partial n/\partial w$, v, and $\partial v/\partial w$ presented in the Experimental section. Similar measurements were also made on biphasic mixtures, using solution columns somewhat longer than those for the isotropic solutions.

In what follows, we express Z_X (X=LS, SED) in terms of the polymer volume fraction ϕ defined by

$$\phi=wv_p/[wv_p+(1-w)v_0] \quad (6)$$

where v_p is the partial specific volume of the polymer at infinite dilution and v_0 the specific volume of the pure solvent; $v_p=0.619\,cm^3\,g^{-1}$,[7] and $v_0=1.0029\,cm^3\,g^{-1}$. Thus, we use the quantities $[\partial\Delta\mu_0/\partial\phi]_X$ defined by

$$[\partial\Delta\mu_0/\partial\phi]_X=Z_X(\partial w/\partial\phi) \quad (X=\text{LS, SED}) \quad (7)$$

EXPERIMENTAL RESULTS

Light Scattering Data

Figure 2 shows the scattering angle θ dependence of n^2/R_θ for light of wavelength 546 nm at different polymer concentrations. It can be seen that the data points at each concentration are fitted closely by a straight line, allowing an accurate estimation of the ordinate intercept n^2/R_0 to be made, where n is

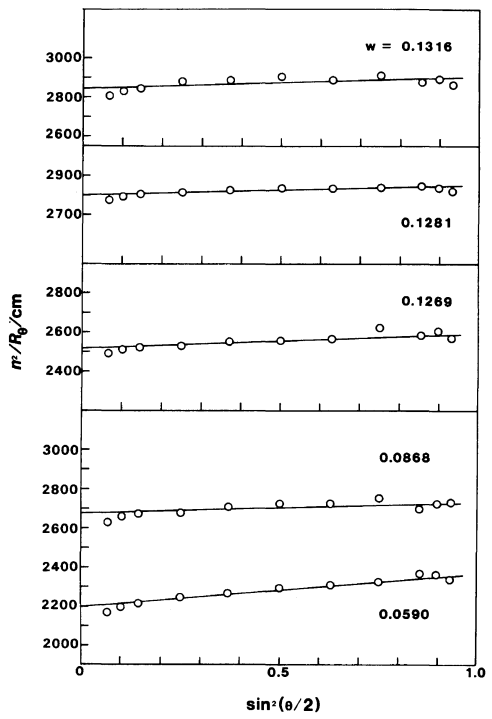

Figure 2. Plots of n^2/R_θ for light of wavelength 546 nm *vs.* $\sin^2(\theta/2)$ for isotropic solutions of sample R23 at 25°C.

Table I. Light scattering data for aqueous solutions of R23 at 25°C

w	ϕ	546 nm				436 nm			
		n^2/R_0	$\langle S^2\rangle_{app}^{1/2}$	$-[\partial\Delta\mu_0/\partial\phi]_{LS}$	$-[\partial\Delta\mu_0/\partial\phi]_{Mn}$	n^2/R_0	$\langle S^2\rangle_{app}^{1/2}$	$-[\partial\Delta\mu_0/\partial\phi]_{LS}$	$-[\partial\Delta\mu_0/\partial\phi]_{Mn}$
		cm	nm	J mol^{-1}	J mol^{-1}	cm	nm	J mol^{-1}	J mol^{-1}
0.0590	0.0373	2190	34	198	207	900	36	200	209
0.0868	0.0554	2670	25	362	370	1075	26	365	373
0.1269	0.0823	2510	34	531	539	1010	38	532	540
0.1281	0.0831	2800	29	597	605	1080	32	575	583
0.1316	0.0855	2480	33	627	635	1120	26	616	624

the refractive index of the solution. The resulting values of R_0 are used to calculate Z_{LS} by the procedure described in the previous section. The data at 436 nm showed substantially the same trend as those at 546 nm and analyzed in the same way. The numerical data of Z_{LS} for sample R23 are summarized in Table I. The values of Z_{LS} at 546 and 436 nm agree with each other, except for the case of $w=0.1281$.

From the slope S_0 of the straight line in Figure 2 we calculated the quantity $\langle S^2\rangle_{app}$ defined by

$$\langle S^2\rangle_{app}=3c\lambda_0^2 M_w K_c S_0/(16\pi^2 n^2) \quad (8)$$

where c is the mass concentration of the polymer and K_c is equal to K with $\partial n/\partial w$ replaced by $\partial n/\partial c$. $\langle S^2\rangle_{app}$ reduces to the mean-square radius of gyration of the polymer, $\langle S^2\rangle_z$ at infinite dilution. It can be seen in Table I that the values of $\langle S^2\rangle_{app}$ are close to 33 nm, which is the $\langle S^2\rangle_z$ value interpolated at the sample's M_w from the $\langle S^2\rangle_z - M_w$ relationship of Kashiwagi *et al.*[16] This agreement may be taken to guarantee the accuracy of R_θ. Indeed, our experience showed that $\langle S^2\rangle_{app}$ was larger for larger R_θ, indicating that optical purification was not satisfactory in such a case.

Sedimentation Equilibrium Data for Isotropic Solutions

Sedimentation equilibrium measurements on isotropic solutions of samples R23, D40, and SPG-3′ were performed using relatively short solution columns and low rotor speeds, so that centrifugal fractionation might be minimized. The results obtained at different rotor speeds agreed with each other within the experimental error. The results are given in Tables II through IV.

Chemical Potential of the Solvent

According to Flory and Abe,[17] the chemical potential of the solvent in an isotropic solution of polydisperse rods is expressed as

$$\Delta\mu_0=RT[\ln(1-\phi)+(1-1/x_n)\phi+\chi\phi^2] \quad (9)$$

where x_n is the number-average axial ratio and χ is the interaction parameter which may depend on ϕ: $\chi=0$ for an athermal solution. Except for some trivial terms, this expression and those for the solute chemical potentials are the same as their counterparts for isotropic solutions of flexible polymers. Therefore, we use Scholte's methods[13,14] for flexible polymers to obtain the solvent chemical potential from light scattering and sedimentation equilibrium data.

His method utilizes the relation:

$$[\partial\Delta\mu_0/\partial\phi]_{Mn}=[\partial\Delta\mu_0/\partial\phi]_X - RTM_0(1/M_n-1/M_w)(\partial w/\partial\phi) \quad (X=\text{LS, SED}) \quad (10)$$

where the subscript Mn indicates that the differentiation is performed at fixed M_n. This relation shows that both light scattering and sedimentation equilibrium measurements should give the same information, *i.e.*, $Z_{LS}=$

Table II. Sedimentation equilibrium data for concentrated isotropic solutions of sample R23 at 25°C

w	ϕ	Rotor speed / rpm	dn/dr / 10^{-3} cm^{-1}	$-[\partial\Delta\mu_0/\partial\phi]_{SED}$ / J mol^{-1}	$-[\partial\Delta\mu_0/\partial\phi]_{Mn}$ / J mol^{-1}
0.059	0.0373	4400	8.69	210	219
0.0868	0.0554		8.44	331	339
0.1281	0.0831		8.09	527	535

Table III. Sedimentation equilibrium data for isotropic solutions of sample D40 at 25°C

w	ϕ	Rotor speed / rpm	dn/dr / 10^{-3} cm^{-1}	$-[\partial\Delta\mu_0/\partial\phi]_{SED}$ / J mol^{-1}	$-[\partial\Delta\mu_0/\partial\phi]_{Mn}$ / J mol^{-1}
0.0196	0.0122	2980	3.88	69.8	74.4
0.0321	0.0200		4.13	108	113
0.0494	0.0311	2980	4.28	165	169
		3370	5.42	163	167
0.0618	0.0391	2980	4.11	216	220
0.0712	0.0452		4.14	251	255
0.0794	0.0505		4.07	286	290
0.0905	0.0579		4.10	327	331

Table IV. Sedimentation equilibrium data for isotropic solutions of sample SPG-3′ at 25°C

w	ϕ	Rotor speed / rpm	dn/dr / 10^{-3} cm^{-1}	$-[\partial\Delta\mu_0/\partial\phi]_{SED}$ / J mol^{-1}	$-[\partial\Delta\mu_0/\partial\phi]_{Mn}$ / J mol^{-1}
0.0246	0.0153	3370	3.43	129	143
0.0249	0.0155		3.65	122	136
0.0503	0.0316		4.21	218	231
0.0700	0.0444		4.29	303	316
0.0745	0.0473		4.36	318	331
0.0981	0.0629		4.19	445	458
0.1082	0.0697		4.07	509	522
0.1285	0.0834		3.82	654	667
0.1539	0.1009		3.80	801	813

Z_{SED}.

In our analysis, M_w/M_n was assumed to be 1.25 for all the samples.[18] The schizophyllan triple helix was approximated by a uniform cylinder of the diameter d, and the axial ratio x_n was calculated from M_n by

$$x_n = M_r v_p/(N_A \pi d^3/4) \qquad (11)$$

Here, as mentioned in the Introduction, d was taken to be 1.67 nm to be consistent with the helix geometry.[7,8] The molecular weight M_0 of the solvent was calculated from the relation: $M_0 = (N_A \pi d^3/4)/v_0$ to be 2210. The values obtained for $[\partial\Delta\mu_0/\partial\phi]_{Mn}$ are summarized in Tables II through IV. As seen in these tables, the polydispersity correction expressed by the

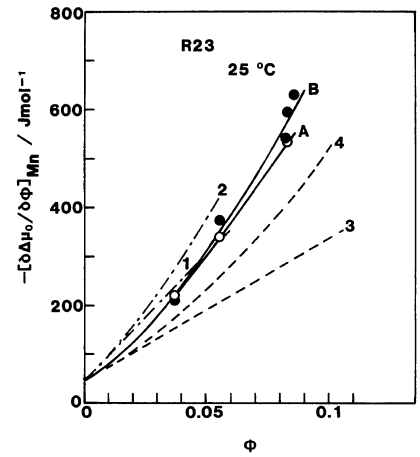

Figure 3. Plot of $-[\partial\Delta\mu_0/\partial\phi]_{Mn}$ *vs.* ϕ for isotropic solutions of sample R23 at 25°C. Unfilled circles, sedimentation equilibrium data; filled circles, light scattering data. Solid curve B, calculated from the Flory–Abe theory (eq 9) with eq 17 and $x_n = 54.7$; solid curve A, with eq 16 and $x_n = 54.7$. Dot-dash curves 1 and 2, calculated for $x = 54.7$ from the Onsager and Cotter theories, respectively; dashed curves 3 and 4, for $x = 29.3$ (see the text). Each of the theoretical curves 1—4 is terminated at ϕ_A, the polymer volume fraction at the isotropic-biphasic boundary.

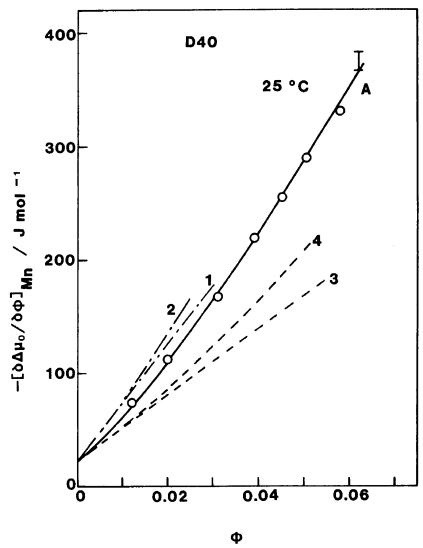

Figure 4. Dependence of $-[\partial\Delta\mu_0/\partial\phi]_{Mn}$ on ϕ for sample D40 at 25°C. Solid curve A, calculated by eq 9 with eq 14 and $x_n = 107$; dot-dash curves 1 and 2, calculated for $x = 107$ from the Onsager and Cotter theories; dashed curves 3 and 4, for $x = 59.4$ (see the text).

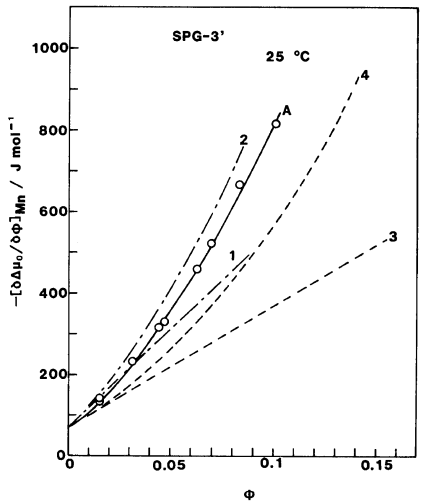

Figure 5. Dependence of $-[\partial\Delta\mu_0/\partial\phi]_{Mn}$ on ϕ for sample SPG-3′ at 25°C. Solid curve A, calculated by eq 9 with eq 15 and $x_n = 35.5$; dot–dash curves 1 and 2, calculated for $x = 35.5$ from the Onsager and Cotter theories; dashed curves 3 and 4, for $x = 19.2$ (see the text).

second term on the right-hand side of eq 10, which is not very appreciable even at small ϕ, becomes rapidly negligible with increasing ϕ.

Figure 3 shows the values of $[\partial\Delta\mu_0/\partial\phi]_{Mn}$ for sample R23 as a function of ϕ. The light scattering (filled circles) and sedimentation equilibrium (unfilled circles) data are consistent with each other but, not exactly. The discrepancy is more conspicuous at higher concentrations, but the reason is not clear. Figures 4 and 5 show plots of $[\partial\Delta\mu_0/\partial\phi]_{Mn}$ for the samples D40 and SPG-3′.

DISCUSSION

Interaction Parameter

As mentioned in the Introduction, concentrated aqueous schizophyllan may be characterized by a non-vanishing interaction parameter χ in the framework of the Flory theory. For simplicity, we assume that $\chi(\phi)$ is expanded by a polynomial in ϕ as

$$\chi(\phi) = \chi_0 + \chi_1\phi + \chi_2\phi^2 + \chi_3\phi^3 \qquad (12)$$

where χ_i ($i = 0$—3) are coefficients dependent

on temperature. As is well known, χ_0 is related to the sedimentation second virial coefficient A_2 of the solution by

$$A_2=(v_p^2/M_0v_0)(1/2-\chi_0) \tag{13}$$

Substitution of eq 12 into eq 9 followed by differentiation with respect to ϕ gives an explicit expression in ϕ for $[\partial\Delta\mu_0/\partial\phi]_{Mn}$. Fitting experimental data for $[\partial\Delta\mu_0/\partial\phi]_{Mn}$ to this expression allows the χ_i coefficients to be evaluated. This was done for the three sets of sedimentation equilibrium data, and the following results were obtained:

$$\chi(\phi)=-0.107-9.33\phi+70.0\phi^2-204\phi^3$$
(D40) (14)

$$\chi(\phi)=-0.055-11.41\phi+66.9\phi^2-228\phi^3$$
(SPG-3′) (15)

$$\chi(\phi)=-0.021-9.03\phi+42.7\phi^2-55\phi^3$$
(R23) (16)

where χ_0 in each equation has been determined from available experimental data for A_2 by eq 13. A similar analysis was performed on the light scattering data for R23, yielding

$$\chi(\phi)=-0.021-9.16\phi+38\phi^2-75.9\phi^3$$
(R23) (17)

Figure 6 shows χ plotted against ϕ. For any sample, $\chi(\phi)$ is negative and decreases monotonously with increasing ϕ. For sample R23,

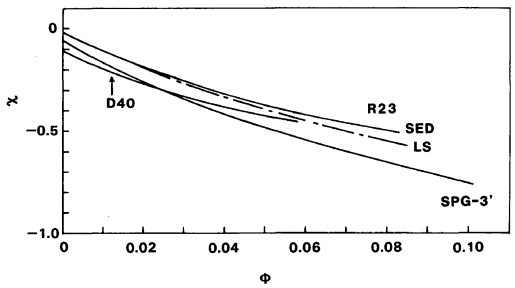

Figure 6. Plots of $\chi(\phi)$ *vs.* ϕ for aqueous schizophyllan at 25°C. Solid curves, determined from the sedimentation equilibrium data; dot–dash curve, from the light scattering data.

the values of $\chi(\phi)$ obtained from the two different methods are in good agreement. Differences in χ among the three samples are not appreciable, where comparison can be made. The thick curves (A) in Figures 3 through 5 represent $[\partial\Delta\mu_0/\partial\phi]_{Mn}$ calculated with the $\chi(\phi)$ given by eq 14—16. They fit the experimental data closely. It is concluded from these findings that the system schizophyllan+water is not athermal in the framework of the Flory–Abe theory.

Comparison with Other Theories

The theory of Onsager[1] is concerned with an imperfect gas of cylindrical particles. It should be valid for long cylinders in dilute solution, but its validity at higher concentration may be questioned, since it relies on a free energy expression linear in ϕ. Note that no such limitation exists in the Flory theory.[3,17] Various attempts have been made to extend the Onsager theory to higher concentration.[19-21] Recently, Cotter[4] has modified the Onsager theory using the scaled particle theory[22] and Lasher's calculation for the phase boundary concentrations.[19] We here confine ourselves to the Onsager theory with no intermolecular interaction and the Cotter theory in analyzing experimental data.

According to these theories, the excess chemical potential $\Delta\mu_0$ of the solvent is expressed in terms of the axial ratio x, the volume fraction ϕ, and the molar volume V_p of the polymer as follows:

$$\Delta\mu_0=-\frac{RTM_0v_0}{V_p}f(x,\phi) \tag{18}$$

Different $f(x,\phi)$ are used by different authors. The theories of Onsager and Cotter give the same expression for the second virial coefficient:[23]

$$A_2=\left(\frac{3x^2+6x-1}{3x-1}\right)\left(\frac{v_p^2}{V_p}\right) \tag{19}$$

To a first approximation, we used the number averages of V_p and x (x_n) to compute $\Delta\mu_0$

given by eq 18; x_n was calculated by eq 11. In Figures 3 through 5 our schizophyllan data are compared with the predictions of the two theories under consideration; the theoretical curves indicated by the dot–dash lines (curves 1 and 2) are terminated at the respective A-point. The linear dependence predicted by the Onsager theory is not in agreement with the experimental data. On the other hand, the values calculated by the Cotter theory are rather close to the experimental data for sample SPG-3′. The theoretical values tend to deviate progressively upward from the data as the molecular weight is increased. Use of the corresponding weight averages[23] for analyzing $[\partial\Delta\mu_0/\partial\phi]_X$ (X=LS, SED) led to a similar conclusion.

Kubo and Ogino[5,6] showed that their osmotic pressure data for the system poly(γ-benzyl L-glutamate) + dimethylformamide agreed with the prediction of the Cotter theory, when x was calculated from A_2 by eq 19. The dashed curves (3 and 4) in Figures 3—5 represent the theoretical values calculated with x obtained in the same way. In contrast with the Kubo and Ogino case, no satisfactory agreement between theory and experiment is seen.

Finally, we used x_w for x in eq 18, which is obtained by $x_w = M_w/(dM_L)$ and d taken to be 2.6 nm, the hydrodynamic diameter of the schizophyllan triple helix.[7,8] The values of $[\partial\Delta\mu_0/\partial\phi]_{Mn}$ computed by the Cotter theory[4] with x thus obtained are shown in Figure 7. The agreement between theory and experiment is excellent. However, it must be noted that the experimental w_A for D40 is 1.7 times as large as the theoretical w_A. This discrepancy cannot be attributed to chain flexibility, against the argument of Kubo an Ogino,[5,6] since the triple helix in this range of molecular weight is completely rigid.[7,8] Thus, the above agreement between calculated and experimental values of $[\partial\Delta\mu_0/\partial\phi]_{Mn}$ does not necessarily support the validity of the Cotter theory. A similar discrepancy in the phase boundary concentration

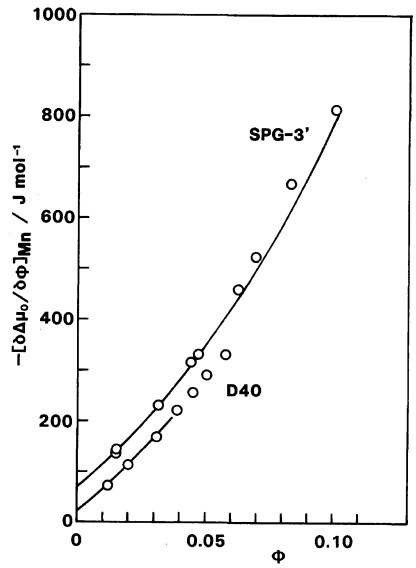

Figure 7. Dependence of $-[\partial\Delta\mu_0/\partial\phi]_{Mn}$ on ϕ for isotropic solutions of samples D40 and SPB-3′ at 25°C. Solid curves, calculated from the modified Cotter theory with x=85.4 for D40 and 28.5 for SPG-3′.

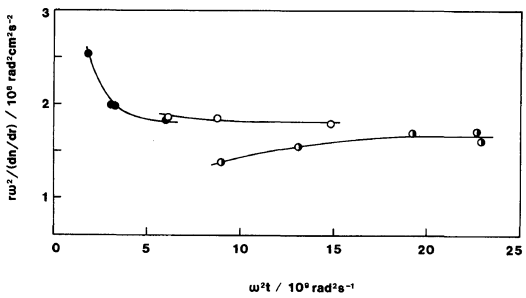

Figure 8. Plots of $r\omega^2/(dn/dr)$ *vs.* $\omega^2 t$ for isotropic phases in biphasic mixtures with different overall concentration ϕ^0. Unfilled circles, ϕ^0=0.0678, the rotor speed=2980 rpm; filled circles, ϕ^0=0.0719, 1980 rpm; half-filled circles, ϕ^0=0.0805, 2200 rpm.

is seen also in the analysis of Kubo and Ogino. In conclusion, neither Onsager theory nor Cotter theory can explain our data satisfactorily.

Chemical Potential in the Biphasic Region

When centrifuged at a rotor speed above 2000 rpm, an aqueous solution of sample D40 in the biphasic region separated into two lay-

Table V. Sedimentation equilibrium data for biphasic solutions of sample D40 at 30°C

w^0	ϕ^0	Rotor speed / rpm	Isotropic phase		Cholesteric phase	
			$\omega^2 r/(dn/dr)$	$-[\partial\Delta\mu_0/\partial\phi]_{SED}$	$\omega^2 r/(dn/dr)$	$-[\partial\Delta\mu_0/\partial\phi]_{SED}$
			10^8 rad^2 cm^2 s^{-2}	J mol^{-1}	10^8 rad^2 cm^2 s^{-2}	J mol^{-1}
0.1001	0.0644	2200	1.79	372	—	—
0.1055	0.0678	2980	1.79	371	—	—
		5560	1.81	376	—	—
0.1115	0.0719	1980	1.81	376	—	—
		2980	1.84	382	—	—
		5560	1.79	371	—	—
0.1192	0.0771	2200	—	—	0.92_0	262
0.1242	0.0805	2200	1.68	349	0.86_0	245

ers, isotropic and cholesteric phases. Observation by a schlieren optical system revealed that the isotropic phase appeared on top of the cholesteric phase with a wide meniscus between the two phases. The volume ratio of the two phases changed very gradually with time, suggesting that it would take quite a long time to attain a true equilibrium state. It was always possible to observe a schlieren pattern in the isotropic phase, and dn/dr could be determined as a function of r. The values of dn/dr were extrapolated to the meniscus between the two phases, r_m. Figure 8 shows $r\omega^2/(dn/dr)$ at r_m plotted against $\omega^2 t$ at different overall concentrations ϕ^0, where t is the time elapsed after the start of centrifugation. It can be seen that within a relatively short period of time $r\omega^2/(dn/dr)$ reaches an equilibrium value which does not depend appreciably on ϕ^0. From these equilibrium values of $\omega^2/(dn/dr)$, Z_{SED} at r_m were calculated on the assumption that $w(r_m)$ equals the A-point concentration at 30°C, *i.e.*, $w(r_m)=0.0965$.[11] The numerical results obtained are summarized in Table V. Note that they satisfy the requirement that Z_{SED} should be independent of the rotor speed.

It was possible to observe schlieren patterns of the cholesteric phase for two solutions of higher concentrations. Values of Z_{SED} at the meniscus in the cholesteric phase were deter-

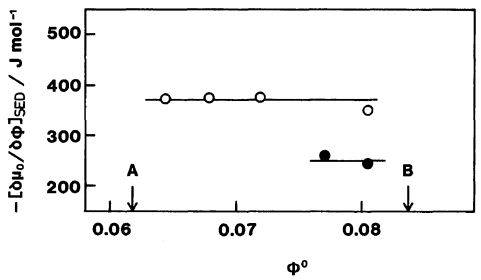

Figure 9. Plots of $-[\partial\Delta\mu_0/\partial\phi]_{SED}$ *vs.* ϕ^0 for biphasic mixtures at 30°C. Unfilled circles, isotropic phases; filled circles, cholesteric phases.

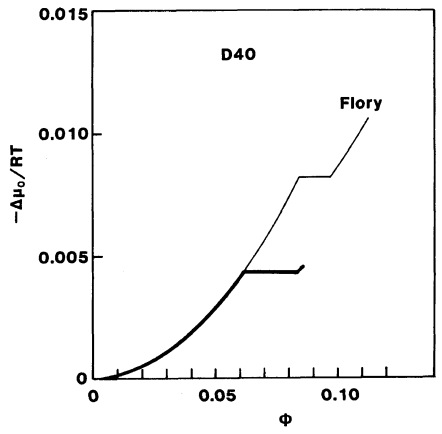

Figure 10. Excess chemical potential $\Delta\mu_0$ of the solvent as a function of ϕ for sample D40. Thick solid curve, experiment; thin curve, the Flory theory.[3]

mined by assuming that $w(r_m)$ in the cholesteric phase was equal to the B-point concentration, 0.129.[11] The numerical results are also given in Table V.

Figure 9 shows $[\partial\Delta\mu_0/\partial\phi]_{SED}$ at the meniscus plotted against ϕ^0, where the arrows A and B indicate the A- and B-points, respectively. It can be seen that, in either phase, $[\partial\Delta\mu_0/\partial\phi]_{SED}$ is almost constant; $[\partial\Delta\mu_0/\partial\phi]_{SED} = -375\,J\,mol^{-1}$ in the isotropic phase and $-250\,J\,mol^{-1}$ in the cholesteric phase. If it is assumed that the chemical potential of the solvent does not depend appreciably on temperature, these data may be compared with those for isotropic solutions at 30°C. Figure 4 shows that the latter can be smoothly extrapolated to the meniscus value (vertical segment).

Integration of $[\partial\Delta\mu_0/\partial\phi]_{Mn}$ by ϕ along with the meniscus value and eq 14 provides $\Delta\mu_0$ as a function of ϕ; the result is shown in Figure 10. The thin curve represents the Flory theory with the non-vanishing χ given by eq 14. The agreement between theory and experiment is not satisfactory because of the disagreement in phase boundary concentration.

REFERENCES

1. L. Onsager, *Ann. N. Y. Acad. Sci.*, **51**, 627 (1947).
2. A. Ishihara, *J. Chem. Phys.*, **19**, 1142 (1951).
3. P. J. Flory, *Proc. R. Soc., London, Ser. A*, **234**, 73 (1956).
4. M. A. Cotter, *Phys. Rev. A.*, **10**, 629 (1974).
5. K. Kubo and K. Ogino, *Mol. Cryst. Liq. Cryst.*, **53**, 207 (1979).
6. K. Kubo, *Mol. Cryst. Liq. Cryst.*, **74**, 71 (1981).
7. T. Norisuye, T. Yanaki, and H. Fujita, *J. Polym. Sci., Polym. Phys. Ed.*, **18**, 547 (1980).
8. T. Yanaki, T. Norisuye, and H. Fujita, *Macromolecules*, **13**, 1462 (1980).
9. K. Van, T. Norisuye, and A. Teramoto, *Mol. Cryst. Liq. Cryst.*, **78**, 123 (1981).
10. K. Van and A. Teramoto, *Polym. J.*, **14**, 999 (1982).
11. T. Itou, K. Van, and A. Teramoto, *J. Appl. Polym. Sci.*, in press.
12. B. H. Zimm, *J. Chem. Phys.*, **14**, 164 (1946).
13. Th. G. Scholte, *J. Polym. Sci., A-2*, **8**, 841 (1970).
14. Th. G. Scholte, *Eur. Polym. J.*, **6**, 1063 (1970).
15. Z_X (X=LS, SED) refers to a given amount of the solvent. Therefore, M_0 is the molecular weight of the "equivalent solvent" corresponding to this amount and does not necessarily equal that of water.
16. Y. Kashiwagi, T. Norisuye, and H. Fujita, *Macromolecules*, **14**, 1220 (1981).
17. P. J. Flory and A. Abe, *Macromolecules*, **11**, 1119 (1978).
18. This value of M_w/M_n was obtained from the observed M_z/M_w by assuming that the molecular weight distribution of each sample was of the Schulz type.
19. G. Lasher, *J. Chem. Phys.*, **53**, 4141 (1970).
20. J. P. Straley, *Mol. Cryst. Liq. Cryst.*, **22**, 333 (1973).
21. M. A. Cotter, *J. Chem. Phys.*, **66**, 1098 (1977).
22. H. Reiss, H. L. Frisch, and J. L. Lebowitz, *J. Chem. Phys.*, **31**, 369 (1959).
23. It can be shown on the basis of the Onsager theory that for a polydisperse sample, the light scattering and sedimentation equilibrium second virial coefficients are related to M_w, whereas the osmotic one to M_n. However, there is no method for evaluating the polydispersity effect on $[\partial\Delta\mu_0/\partial\phi]_X$ (X=LS, SED) at high concentration. Thus, it is a reasonable first approximation to use the same type of average for V_p and x in eq 18 to compute theoretical values of $\Delta\mu_0$.